Proceedings Paper:
Boyle, H., Norgren, S., Crawforth, P. et al. (2023) Insights in α-Al2O3 degradation in multilayer CVD coated carbide tools when turning IN718. In: Hanke, S., (ed.) Wear. 24th International Conference on Wear of Materials, 16-20 Apr 2023, Banff, Canada. Elsevier BV. Article no: 204786. ISSN: 0043-1648. EISSN: 1873-2577.

https://doi.org/10.1016/j.wear.2023.204786

Wear 523 (2023) 204786

Contents lists available at ScienceDirect

Wear

journal homepage: www.elsevier.com/locate/wear

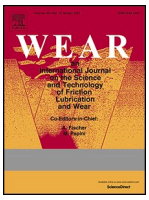

Insights in α-Al2O3 degradation in multilayer CVD coated carbide tools when turning IN718

Henry Boyle [a,*], Susanne Norgren [b,c], Pete Crawforth [d], Katerina Christofidou [a], Denis Boing [b], Martin Jackson [a]

[a] Department of Materials Science and Engineering, The University of Sheffield, Mappin Street, Sheffield, S1 3JD, UK
[b] AB Sandvik Coromant R&D, Lerkrogsv. 13, 126 80, Stockholm, Sweden
[c] Division of Production and Materials Engineering, Lund University, Lund, Sweden
[d] Advanced Manufacturing Research Centre, Advanced Manufacturing Park, Catcliffe, Rotherham, S60 5TZ, UK

ARTICLE INFO

Keywords:
CVD
Textured alumina
Superalloy
Machining

ABSTRACT

The degradation behaviour of textured CVD α-alumina has received significant attention within academic literature with regard to steel turning. In contrast, the research performed on Ni-based superalloys is yet to be brought up to the same level of understanding. Hence, the objective of this report will be to offer insights with regard to the degradation mechanisms of the textured alumina layer of CVD Ti(C,N)/α- Al_2O_3 coated carbides when turning a Ni-based superalloy, and to explore the role of different wear mechanisms that contribute to cutting tool failure. Adhesive wear was observed to be the primary wear mechanism responsible for coating failure, which can result in sudden mechanically driven grain pull-out and delamination events. Grain-pull out was observed across the entire contact zone; delamination was observed to occur most frequently around the trailing edge and depth-of-cut notches, and towards the end of the contact zone as the chip separates from the tool. Evidence of characteristic plastic deformation induced ridges in the alumina coating surface were also revealed within the sliding zone, leading to gradual wear of the alumina layer. These findings demonstrate that there are both similarities and differences in alumina degradation behaviour when compared to previous studies conducted on steel turning.

1. Introduction

Within machining, coatings are commonly used to protect an underlying hardmetal substrate from abrasive, chemical, diffusive and adhesive wear mechanisms, and to enhance the tool performance due to degradation resistance of the coating itself. The types of wear a cutting edge is subjected to may be heavily time dependent, and can evolve across the course of a machining operation e.g., crater wear, flank wear, notch wear. Compared to other metallic systems, Ni-based superalloys exhibit low thermal conductivities, which leads to high thermal gradients in the cutting zone and contributes significantly to the acceleration of thermally driven tool wear phenomena [1]. Workpiece adhesion and work hardening are also especially severe, which leads to coating delamination and contributes to depth-of-cut (DOC) notch wear [2]. In addition, the presence of hard abrasive particles within the microstructure can also contribute to the occurrence of abrasive wear [3]. Typically, tool wear studies are carried out by wearing a given tool until it reaches end of tool life. The tool life is a function that is dependent on the wear behaviour and interaction of each coating layer, and the substrate itself. To develop cutting tools for specific materials, it is necessary to investigate the degradation of each of these separate components. This can effectively be achieved for the outermost coating layers by employing short times in cut to investigate the initiation of tool wear. Understanding this behaviour is essential, as it will dictate the subsequent wear progression.

Various tool materials have been explored for machining Ni-based superalloys. Ceramic tools are commonly used for continuous roughing operations requiring a high material removal rate and high cutting speeds, permitted by their high melting temperatures and hot hardness [1]. For semi-finishing and finishing operations, coated carbides (PVD [4] and CVD [5]) as well as cBN [4,6] tools are preferred. Due to its chemical inertness, high temperature stability, hardness and wear resistance, CVD alumina coatings have been found to be well suited to the conditions that develop during Ni-based superalloy machining and

* Corresponding author.
E-mail address: hrboyle1@sheffield.ac.uk (H. Boyle).

https://doi.org/10.1016/j.wear.2023.204786
Received 28 September 2022; Received in revised form 17 December 2022; Accepted 12 January 2023
Available online 22 March 2023

are commonly used in combination with other wear resistant coatings such as Ti(C,N) to form a multi-layer coating [7]. Since these coatings were developed for steel machining, much of the published work on alumina degradation mechanisms are focused solely on steel. The majority of research regarding the wear behaviour of CVD Ti(C,N)/Al_2O_3 coated carbides when machining Ni-based superalloys has centred on the performance of both the coating and insert, and not solely on the alumina layer.

The dominant wear types in CVD Ti(C,N)/Al_2O_3 coated carbides when turning Inconel 825 have been reported to be abrasion and adhesion, leading to edge chipping and nose wear during dry machining [5]. Compared to PVD coated tools, such as TiAlN and TiN, the CVD coating was found to produce higher temperatures, greater dynamic fluctuation in machining force signals and increased built up edge (BUE) formation. During turning of IN718 it has been shown that CVD Ti(C,N)/Al_2O_3 coated carbide can outperform single-layer (TiAlN) PVD coated carbides at high cutting speeds (100 m/min) but not at medium speeds (75 m/min) [8]. It was also found that the majority of abrasive wear occurs on the tool flank, which the authors claimed was due to hard abrasive particles from the workpiece material. As the abrasive wear was concentrated on the tool flank, it is possible that dislodged sections of the coating/substrate, caused by attrition wear, may also contribute. Kadirgama et al. [9] found that during milling of Hastelloy C–22HS with CVD Ti(C,N)/Al_2O_3 coated carbides, that adhesion, BUE and oxidation of the underlying substrate were the dominant wear mechanisms; the tool failure modes were reported as flank wear, chipping, plastic deformation and notching. Ezugwu et al. reported that flank wear and notching were the dominant failure modes of CVD Ti(C,N)/Al_2O_3 coated carbides when turning IN718, compared to flank wear, excessive chipping and flaking for multilayer/single layer PVD tools [2].

Song et al. [10] investigated the initial wear behaviour of coated and uncoated carbides during dry turning of IN718 When using CVD Ti(C,N)/Al_2O_3 tooling, adhesive wear was identified as the primary wear mechanism. In a similar study on IN718 turning by Rakesh et al. [11], coating delamination and abrasion driven crater wear were identified as wear mechanisms. Again, the authors claim abrasive wear occurred due to the presents of hard abrasive particles in the workpiece but provided no evidence to support this. Diffusive wear is also alleged to have occurred; however, it is not clear how this could be distinguished from adhesive wear given the evidence provided.

Dearnley and Trent [12] first reported on the rake face crater wear of CVD alumina coatings during steel turning, and observed plastic deformation to the asperities of early-stage mixed alumina coatings (which were partially textured, containing both α-alumina and κ-alumina). This resulted in the formation of characteristic ridges parallel to the cutting direction, concentrated in the location of the maximum rake face temperature. These ridges were observed to form most notably when turning at high cutting speeds. Dearnley [13] later suggested that these ridges form via the plastic deformation of coating asperities, which culminates in ductile fracture and material loss of the coating. Goh et al. [14] reported that plastic deformation by single glide of individually spalled grains was responsible for the formation of these long ridges during medium carbon steel turning when using alumina-based ceramic inserts. The authors also claimed plastic deformation induced necking resulted in the formation of short spikes in the surface nearer to the cutting edge, indicating that multiple slip conditions were present in the surface layer of the tool. Furthermore, they suggest the spiked appearance may be caused by partially dislodged or damage grains that are fused onto the tool material before being deformed. Fallqvist et al. [15] used a pin-on-disk tribometer to study wear behaviour of textured α-alumina coatings with different growth textures at high and low temperatures. When using a cast iron pin, they found plastic deformation was the dominant wear type for the (001) growth texture and that micro-chipping occurred when the other growth textures were tested.

During steel machining, it has been demonstrated that the wear resistance of pure α-alumina coatings can be controlled by varying the growth texture. It has been hypothesised when machining steels, that the optimum wear resistance of α-alumina coatings is achieved when the basal plane (001) lies parallel to the substrate surface [16]. M'Saoubi et al. [17] observed that during steel turning, textured α-alumina coatings exhibited three distinct types of wear in the sticking, transition and sliding zones, when machined at high speeds (300 m/min). When machined at moderate speeds (100 m/min), no evidence of characteristic ridges indicative of plastic deformation was observed in the transition or sliding zones. Using energy-dispersive X-ray spectroscopy (X-EDS) to investigate the chemistry of the plastically deformed alumina in the transition zone, it was discovered that Mg containing oxide deposits were formed, possibly originating from non-metallic inclusions in the workpiece material. Bejjani et al. [18] demonstrated that when turning different types of steel workpiece materials with α-alumina coated carbides, that the positions and sizes of each wear zone would vary, as would the topography and wear rate in the transition zone.

Bjerke et al. [19] investigated the performance of CVD α-Al_2O_3 when turning Ca-treated steels. The authors were able to explain the anonymous wear behaviour, in which a reduction in tool life was seen when using CVD α-Al_2O_3 tools despite Ca-treatment leading to a tool life increase when turned using other tool materials such as uncoated carbides [20]. Although commonly regarded as inert, via a combination of microstructural investigations, thermodynamic calculations and temperature measurement, it was demonstrated that the alumina will react at the conditions experienced during machining, and that the degradation was driven by non-metallic inclusion (NMI) and oxides within the workpiece material. In a subsequent work [21] it was shown using high pressure diffusion couples that these kinds of reactions are dependant oxygen. The authors suggested that NMI in engineered steels should be saturated with Al to prevent this chemically driven wear.

Shoja et al. [22] performed an extensive analysis of the crater wear mechanisms that occur during steel turning when using CVD Ti(C,N)/α-Al_2O_3 coated carbide tools with differing alumina growth textures. Chemical wear, plastic deformation, micro-rupture and abrasion were all found to occur during the turning operations. An estimated temperature range of between 950 and 1000 °C was stated by the authors. Nano-scale terraces were observed to form depending on the growth texture used for the coating, furthermore, when investigating previous claims surrounding micron size grooves caused by abrasive wear, no such grooves were observed on the (001) sample. The grooves observed in the other growth textured samples were evenly dispersed across the whole DOC, leading the authors to conclude that any abrasion that does appear is likely caused by micro rupture of alumina that occurs in the sticking zone. Using STEM imaging of the worn coating cross-section, a smooth, flat surface morphology was observed where the (001) sample had undergone plastic deformation.

Coolant can have a significant impact on the wear behaviour observed during machining. Sosa et al. [23] used a cyclic contact fatigue test to investigate the role of coolant on crack propagation in textured α-alumina coatings during milling operations. It was shown that under wet conditions there is a faster widening of the CVD cooling cracks which leads to the development of large comb-cracks and ultimately coating failure. Alagan et al. [24] investigated the impact of simultaneous rake and flank high pressure cooling on chip formation mechanics when turning IN718 with uncoated carbide tools. They found that increasing the rake cooling reduced the chip width and curvature. Flank cooling was found to mainly effect the shear instability and chip breaking. When increasing the cutting speed, the chip thinness and shear angle was observed to increase.

In summation, the state-of-the-art in terms of textured alumina degradation behaviour demonstrated by the contributions previously discussed is not equally distributed across the different workpiece materials. The work conducted on Ni-based superalloys, in comparison to steels, is more rudimental and has not yet been brought up to the same level of understanding. In addition, much of this work has utilised non

Table 1
Composition in wt.% of IN718 workpiece material.

Ni	Cr	Fe	Nb	Mo	Ti	Al	Trace
53.5	18.53	17.8	5.3	3.02	1.06	0.5	0.29

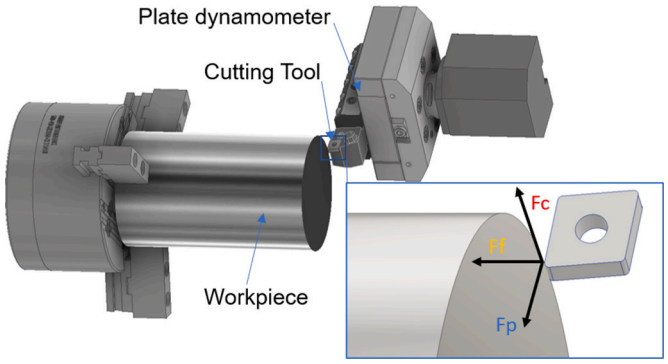

Fig. 1. Diagram of the turning setup used in the machining trial.

textured and mixed (α and κ)-alumina coatings, and not strongly textured α, thus they degrade in a different manner. In the case of steels, it has been shown that many misconceptions surrounding the plastic deformation behaviour of alumina have persisted, and that the chemical inertness of alumina is not as absolute as once believed in steel machining environments. Hence, there is a clear knowledge gap that persists in terms of understanding whether these recent discoveries are relevant when machining radically different materials such as Ni-based superalloys, which are more prone to chemical wear and have a lower thermal conductivity. The objective of this work is to offer initial insights into the degradation mechanisms of the textured alumina layer of CVD Ti(C,N)/α-Al_2O_3 coated carbides when turning IN718, and to contribute to the understanding of the wear mechanisms that lead to the failure of CVD coated cutting tools.

2. Materials and method

2.1. Experimental materials

The workpiece material was solution annealed and aged IN718 (Table 1), with a hardness of 411 HBW, an initial diameter of 120 mm and a length of 202 mm. A QS-PCLNL 2020–12C shank and Sandvik Coromant commercial grade CNMG 12 04 08-SF S205 inserts were used for the experiments. The inserts feature a multilayer CVD coating of Ti (C,N) (5 μm) followed by α-Al_2O_3 (3 μm) on the rake face, whereby the alumina layer is textured in the (001) plane. During manufacture a TiN layer is used to coat the entire insert, this layer is then blasted off the rake face but kept on the flank of the tool, hence, the rake and flank have different coating systems. Prior to the trials, edge rounding measurements were taken of 40 insert cutting edges, 25 inserts within a $\rho = (40 \pm 1)$ μm range were down selected for the trial. The coolant used was Blaser Vasco 7000, a commercial coolant with a pH of 8.5/9 and a concentration of 11.7%.

2.2. Test methods

The experimental machining trials were conducted on an DMG Mori NLX 2500 lathe, the experimental setup is shown in Fig. 1. Longitudinal turning operations were performed over different machined lengths (spiral cut length): 2 m, 32 m and 128 m. A Kistler plate piezoelectric force dynamometer (Type 9129AA) fixed to a capto C5 tool adapter, was used to measure the machining force components during cutting in the radial (x), cutting (y) and feed (z) directions (see Fig. 1); this was done primarily to monitor the edge condition and ensure consistent tool engagements. A sample rate of 20 kHz was selected. Parameters used were chosen to be representative of a standard industrial process. High pressure through tool coolant with a pressure of 65 bar was used for all cuts made. Since coolant properties heavily influence tool wear, pH levels were routinley measured using litmus paper and concentration

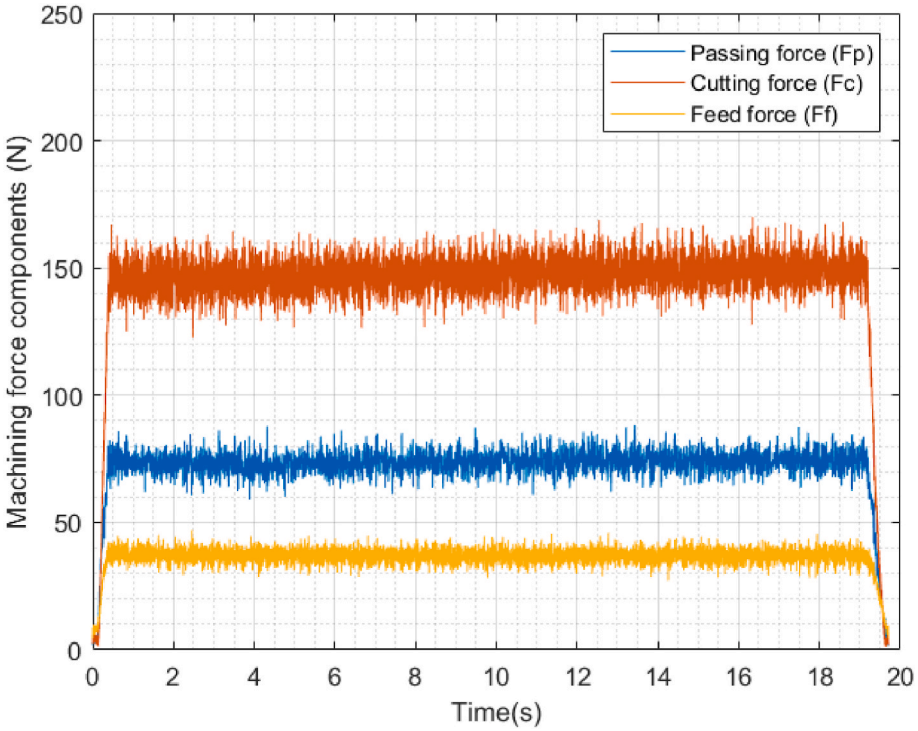

Fig. 2. Machining forces measured: Cutting force (Fc), Feed force (Ff) and Passing Force (Fp), using Kistler piezoelectric plate dynamometer during 32 m machined length test.

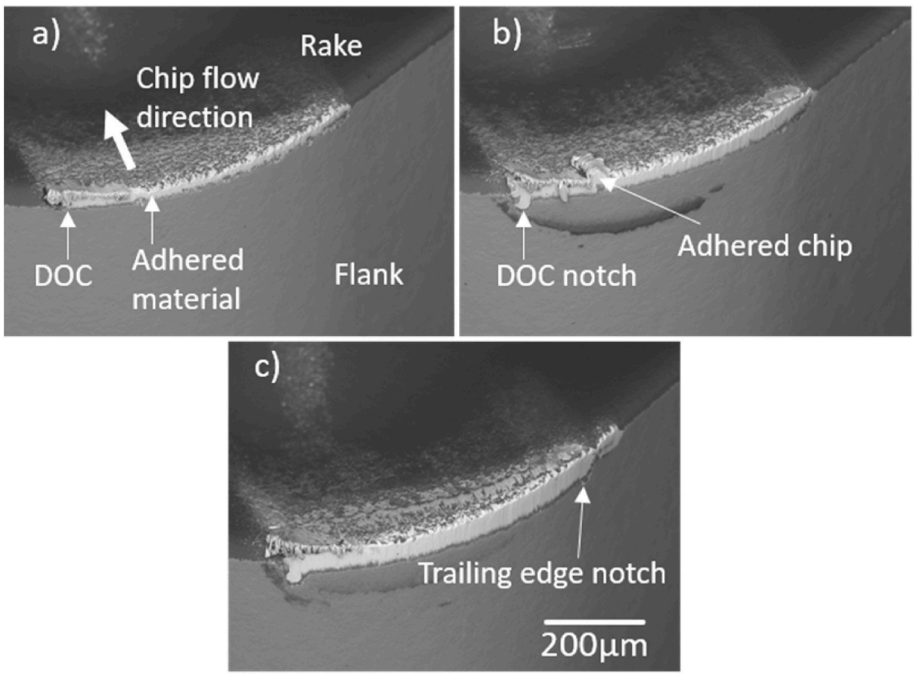

Fig. 3. BSE micrographs of tool wear developed during turning trial at each machined length a) 2 m b) 32 m c) 128 m

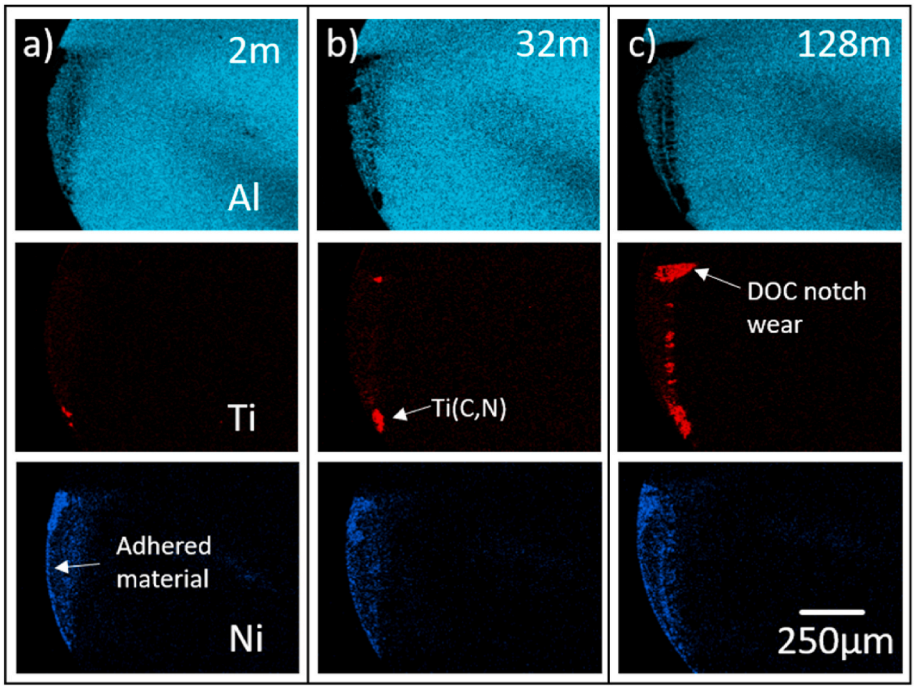

Fig. 4. X-EDS of adhered material on worn inserts for Al, Ti and Ni at different machining times a) 2 m b) 32 m c) 128 m

levels were monitored using a refractometer to ensure they remained consistent throughout the trial. As per the tooling manufacturers recommendations, the DOC used for all cuts was 0.25 mm and the feed rate 0.1 mm/rev. A cutting speed of 100 m/min was employed. Machined lengths of 2 m, 32 m and 128 m were selected for the initial wear trial, which represent 0.2%, 2.7% and 11.7% of tool life respectively (verified by previous tool life trial). Three repeats were conducted for each length.

2.3. Characterisation techniques

Scanning electron microscopy (SEM) was carried out on a Zeiss EVO LS25-1204 and a Hitachi TM3030. Imaging was conducted using a combination of backscattered electron (BSE) and secondary electron (SE) detectors. A 45^{o} holder was used for imaging tool nose wear. An 80 mm Oxford X-EDS system was used to perform compositional analysis. Etched inserts were etched in Glyceregia for approx. 1 h. Average thickness measurements were taken from five separate measurements spaced 10 µm apart across 50 µm sample sections; three repeats were

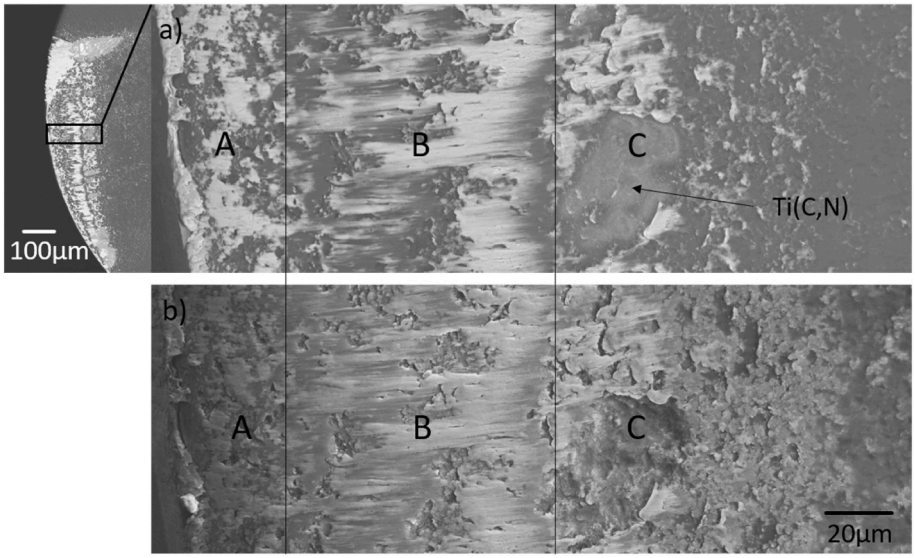

Fig. 5. BSE micrograph of worn unetched sister insert showing adhered material after a machined length of 128 m

taken of each measurement.

3. Results and discussion

An example of the machining forces measured during the experiment is shown in Fig. 2. In all experiments performed the cutting force (Fc) was found to be the largest of all force components, followed by the passing force (Fp) and the feed force (Ff). The smooth gradient during the initial engagement indicates a stable entrance of the tool with no unexpected failure or abrupt wear, similarly there are no large variations during the cut either. The wear observed during the trials is shown after 2 m, 32 m and 128 m turned length in Fig. 3. After 2 m turned length, the workpiece material is adhered to the tool (Fig. 3a). By 32 m, the region covered by adhered material has increased significantly in thickness, a DOC notch and chip adhesion can also be observed (Fig. 3b). After 128 m (Fig. 3c) turned length, the thickness of the adhered material on the cutting edge has increased further. In addition, the DOC notch has continued to expand and a small trailing edge notch has started to develop (Fig. 3c).

Fig. 4 shows X-EDS mapping of the elements Al, Ti, and Ni on the damaged tools after each machined length. The Al signal indicates the alumina coating and so is the majority of the signal seen on the rake of the tool. Ni indicates adhered workpiece material, which has formed or adhered in the tool/chip contact zone. The Ti signal indicates that the Ti (C,N) layer of the coating has now been exposed as the alumina coating has been removed. Fig. 4a shows a small notch/chipped region that has formed after 2 m of turning towards the trailing edge of the tool. The wear may be concentrated in this region as the chip is at its thinnest, meaning the chip compression ratio is higher, and so more work hardening and grain refinement of the workpiece material can be expected. After 32 m (Fig. 4b), the wear in this region continues to expand as the alumina layer is removed, there is also additional exposure of the Ti(C, N) layer around the DOC notch. By 128 m, (Fig. 4c), the alumina layer has worn further in the regions previously displaying wear. Furthermore, the alumina coating wear around the DOC has become significantly enlarged and elongated. Several additional areas of alumina coating failure have also appeared towards the rear of the contact zone as the chip begins to deflect.

In Fig. 5a it is revealed that the strong signals of Ti observed in Fig. 4 are areas where the alumina coating has delaminated; Fig. 5b shows the rough topography of the fractured surface that remains. Three distinct wear zones can be seen in the worn surface. Zone A is the sticking zone, an area that appears to correspond to the edge radius of the tool. Zone B

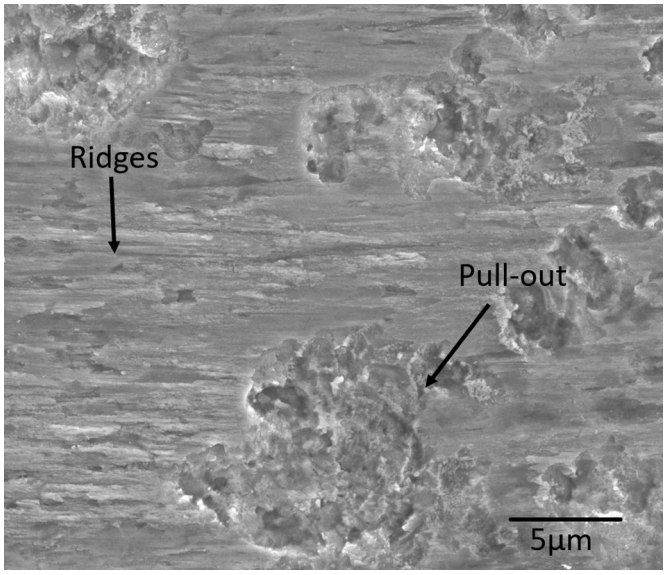

Fig. 6. SE micrograph showing worn surface of etched alumina after 128 m machined length in zone B.

is the sliding zone, distinguished by the smeared adhered workpiece material. There is no clear transition zone observed between zones A and B, potentially due to the small DOC employed. Zone C is the end of contact zone, an area in which there is a transition from the sliding contact of zone B as the chip begins to separate from the tool. In this zone, delamination events occur most frequently (except for the DOC and trailing edge notches), as a result of tensile forces caused by the combination of adhesion and chip deflection [25]. Typically, crater wear occurs some distance behind the cutting edge [12]. The exact position is dependent on the contact pressure, sliding velocity and temperature distribution [26]. In zone C the high-pressure coolant (HPC) on the rake side of the tool forms a hydrodynamic wedge which changes the stress distribution, reducing the size of the contact zone, lowering frictional forces and temperatures. The reduction in pressure in this region may permit the occurrence of coolant driven wear phenomena and oxidation to occur. This behaviour has not been seen during steel turning investigations regarding alumina layer degradation [16–18,22], which may be attributed primarily to the high degree of adhesive wear in

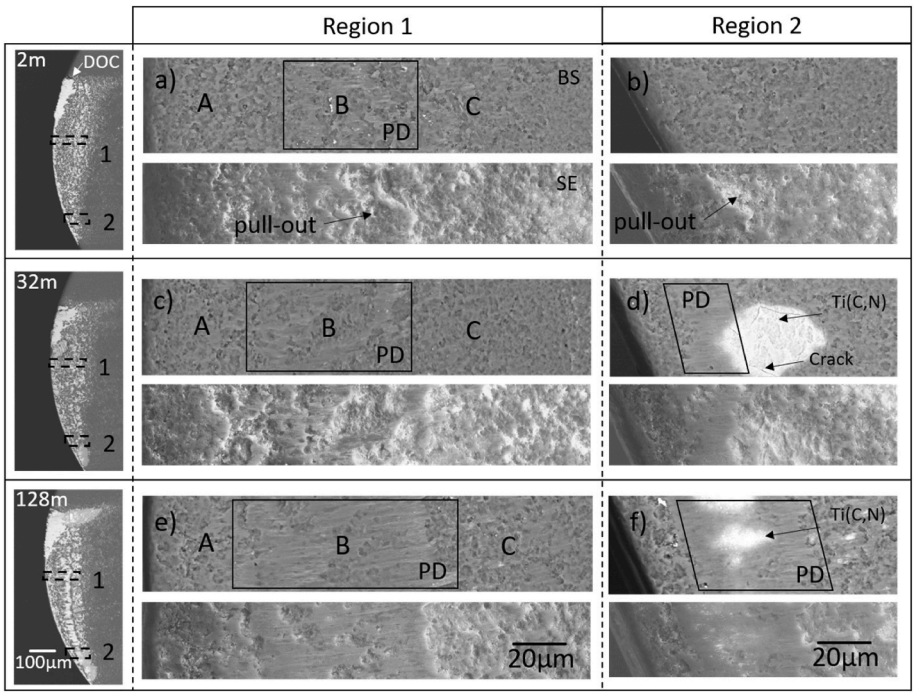

Fig. 7. SEM backscattered electron micrographs showing alumina wear unetched (BSE imaging) and etched (SE imaging) sister inserts compared at different machining times a) region 1 at 2 m b) region 2 at 2 m c) region 1 at 32 m d) region 2 at 32 m e) region 1 at 128 m f) region 2 at 128 m

combination with the effect of HPC and a very reactive workpiece material with low thermal conductivity.

In order to explore the wear mechanisms that alumina is subjected to it is necessary to remove the adhered material using etching techniques. The worn alumina surface of the etched sister insert in the sliding zone (zone B), after 128 m machined length, is presented in Fig. 6. The worn surface exhibits two characteristic distinct wear types: the first type is identified by ridges that have formed on the tool surface, indicative of plastic deformation in the alumina due to slip, which appears to correspond to the smeared material observed in Fig. 5. Plastic deformation of alumina has been widely reported during dry steel turning [16–18,22]. Although no temperature measurements were made during this experiment (since longitudinal turning operations do not permit the use of a thermal camera), maximum rake face temperatures in orthogonal dry Ni-based superalloy turning have been reported to be in the region of 1000 °C [27], which is comparable to those achieved during dry steel turning [28]. Therefore, the likelihood for activation of different slip systems in the alumina coating is expected to be similar. The effect of coolant on the maximum temperature remains disputed as an exact measurement of surface temperatures in the tool-chip contact zone is often not feasible. Thermal modelling suggests that a temperature decrease of between 31 and 38 °C could be expected when using an 80 bar coolant pressure supply when turning IN718 using similar processing parameters to those used in the study [29]. As such, the impact of coolant on maximum temperatures in the contact zone is considered to be minimal.

The second observable wear type shown in Fig. 6 is grain pull-out of the alumina coating. It is hypothesised that coating pull-out is largely controlled by an adhesive wear dominated mechanism that occurs when the bond formed between the alumina and workpiece material has a stronger bonding energy than the intergranular bonding energy of the alumina grains. This in contrast to the observations made during steel turning experiments in which no grain pull-out is observed in the sliding zone [16–18,22].

To study the wear progression during machining, SEM micrographs were taken in both BSE and SE imaging modes of the etched sister inserts at each machined length tested. BSE images were used to indicate when the alumina layer had worn through, as changes in composition will be shown as changes in contrast. SE images were taken to obtain topographical information, in order to determine if grains of the alumina had been pulled out. The etched sister inserts were imaged in two regions: 1 and 2 (see Fig. 7). Region 1 is positioned near middle of the tool, near the average chip thickness. Region 2 is located towards the trailing edge, and so the surface speed is slower than at region 1 as it is closer to the centre of rotation. In addition, the chip is thinner, and therefore the chip compression ratio is higher.

Despite the short time in cut, Fig. 7a demonstrates there is evidence of plastic deformation in region 1 (shown as PD) after a machined length of 2 m, which corresponds to the sliding zone (zone B). In the area displaying plastic deformation there are also indications of coating pull-out; to the left of this region there is an area characterised solely by coating pull-out. This area corresponds to the sticking zone (zone A). Towards the right of the plastically deformed region there are further areas displaying coating pull-out, which lie within the end of contact zone (zone C). In region 2, there appears to be less evidence of plastic deformation (Fig. 7b), although some coating pull-out has occurred.

After 32 m of cutting (Fig. 7c), the plastically deformed area has expanded towards the sticking zone (zone A), potentially due to the temperature increase caused by the longer time in cut. Significant grain pull-out is also observed within the plastically deformed area, as well as to the right in the end of contact zone (zone C). In region 2 after 32 m machined length (Fig. 7d), there is a large delaminated region to the right of the plastically deformed area. The overlap between these two regions appears gradual, demonstrating further plastic deformation of the alumina layer occurred after the delamination event.

After a machined length of 128 m (Fig. 7e), the plastically deformed regions of alumina have increased both towards and away from the cutting edge. It appears as if this wear behaviour has resulted in a smoother topography. Areas exhibiting coating pull-out can be observed within the plastically deformed region, as well as in the sticking zone (zone A) and the crater zone (zone C). In region 2 (Fig. 7f), it appears as if the continued alumina wear via plastic deformation has led to the Ti (C,N) layer becoming partly exposed. This appears to be as a result of a more gradual wear than was observed in Fig. 7d, since the revealed Ti(C,

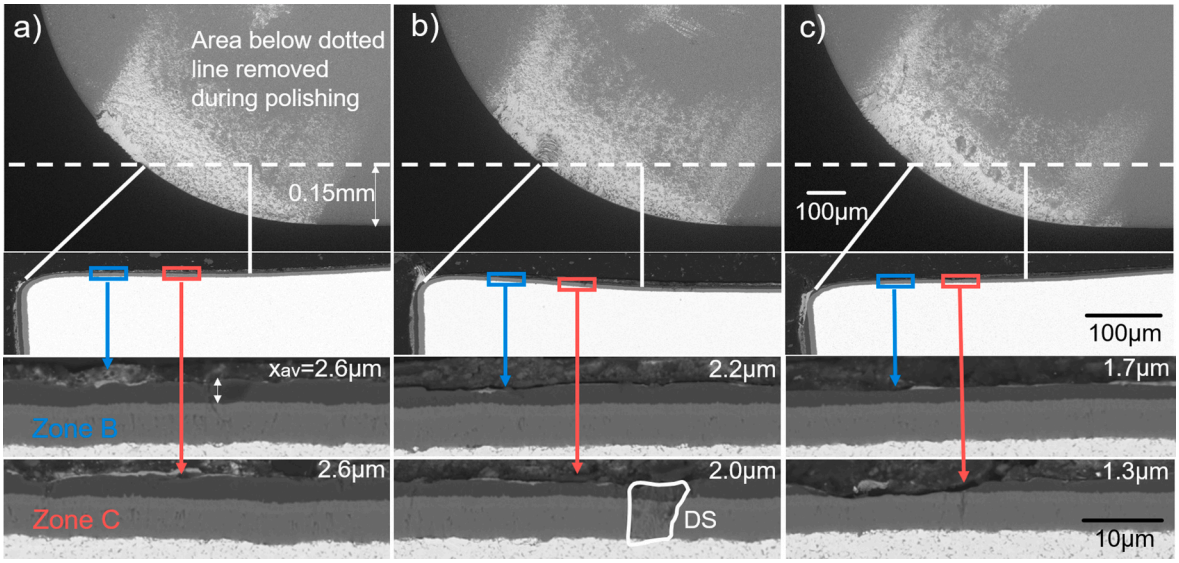

Fig. 8. Cross sections of inserts taken from plastic deformation region and pull-out region at different machining times a) 2 m b) 32 m c) 128 m

N) is contained entirely within the plastically deformed area. This highlights the fact that there is significant variability when observing the wear behaviour, as this gradual wear regime may not be observed if a sudden delamination has already occurred.

Cross sections of the worn tools were metallographically prepared to investigate variations in alumina coating thickness. This was done by polishing away approximately 0.15 mm of material (as shown in Fig. 8). Two separate 50 μm sample regions were chosen to be representative of the sliding zone (zone B), 100–150 μm from the tool edge, and the crater zone (zone C), 200–250 μm from the tool edge; the average coating thickness (x_{av}) is shown for each sample region. After 2 m of cutting (Fig. 8a) it can be observed that both sample regions have a similar appearance in terms of both topography and thickness. A similar observation is made after 32 m of cutting (Fig. 8b), although in zone B, a dislodged section (labelled DS) is observed whereby both the alumina and Ti(C,N) layer have been removed. This may have been caused by the propagation of CVD cooling cracks within the coating during either polishing or machining. After 128 m (Fig. 8c), a noticeable difference in the two regions is revealed, with a large section of alumina (≈20 μm) in zone C being completely removed and the underlying Ti(C,N) layer exposed.

4. Conclusions

- Adhered workpiece material, DOC notching and coating delamination were observed on the worn tools after short machining times.
- Evidence of plastic deformation of the worn alumina surface was detected in the sliding zone, and was observed to expand as the machined length increased.
- Alumina grain pull-out was detected across the entire contact zone, demonstrating the high degree of adhesive wear; this behaviour has not been seen during other studies previously conducted on α-alumina degradation in steel turning.
- Delamination of the alumina layer was observed to occur most frequently at the DOC and trailing edge notches, as well as at the rear of contact zone (zone C).
- Alumina degradation can occur as a result of a sudden mechanically driven delamination or gradual wear facilitated by plastic deformation.

Declaration of competing interest

The authors declare that they have no known competing financial interests or personal relationships that could have appeared to influence the work reported in this paper.

Acknowledgments

This work was supported by Sandvik Coromant, Science Foundation Ireland [18/EPSRC-CDT/3584] and the Engineering and Physical Sciences Research Council UK [EP/S022635/1]. I would also like to thank Christer Fahlgren, Alex Graves and Changhong Xiao for their assistance in obtaining the cross-sectional micrographs.

References

[1] T. Kitagawa, A. Kubo, K. Maekawa, Temperature and wear of cutting tools in high-speed machining of Inconel 718 and Ti-6Al-6V-2Sn, Wear 202 (2) (Jan. 1997) 142–148, https://doi.org/10.1016/S0043-1648(96)07255-9.
[2] E.O. Ezugwu, Z.M. Wang, C.I. Okeke, Tool life and surface integrity when machining inconel 718 with pvd- and cvd-coated tools, Tribol. Trans. 42 (2) (Jan. 1999) 353–360, https://doi.org/10.1080/10402009908982228.
[3] A. Jawaid, S. Koksal, S. Sharif, Wear behavior of pvd and cvd coated carbide tools when face milling inconel 718, Tribol. Trans. 43 (2) (Jan. 2000) 325–331, https://doi.org/10.1080/10402000008982347.
[4] M.A. Xavior, M. Manohar, P. Jeyapandiarajan, P.M. Madhukar, Tool wear assessment during machining of Inconel 718, Procedia Eng. 174 (2017) 1000–1008, https://doi.org/10.1016/j.proeng.2017.01.252.
[5] A. Thakur, S. Gangopadhyay, K.P. Maity, S.K. Sahoo, Evaluation on Effectiveness of CVD and PVD Coated Tools during Dry Machining of Incoloy 825, vol. 59, Nov. 2016, pp. 1048–1058, https://doi.org/10.1080/10402004.2015.1131350, no. 6.
[6] J.P. Costes, Y. Guillet, G. Poulachon, M. Dessoly, Tool-life and wear mechanisms of CBN tools in machining of Inconel 718, Int. J. Mach. Tool Manufact. 47 (7–8) (2007) 1081–1087, https://doi.org/10.1016/j.ijmachtools.2006.09.031. Oxford.
[7] D. Gao, Z. Hao, R. Han, Y. Chang, Performance of alloyed CVD-coated and PVD-coated carbide tools in dry machining nickel based alloy Inconel718, Adv. Mater. Res. 426 (2012) 118–121, https://doi.org/10.4028/WWW.SCIENTIFIC.NET/AMR.426.118.
[8] A. Bhatt, H. Attia, R. Vargas, V. Thomson, Wear mechanisms of WC coated and uncoated tools in finish turning of Inconel 718, Tribol. Int. 43 (5–6) (May 2010) 1113–1121, https://doi.org/10.1016/j.triboint.2009.12.053.
[9] K. Kadirgama, K.A. Abou-El-Hossein, M.M. Noor, K.V. Sharma, B. Mohammad, Tool life and wear mechanism when machining Hastelloy C-22HS, Wear 270 (3–4) (Jan. 2011) 258–268, https://doi.org/10.1016/j.wear.2010.10.067.
[10] X. Song, T. Yukio, I. Tohru, Influence of built-up layer on the wear mechanisms of uncoated and coated carbide tools during dry cutting of Inconel 718, Seimitsu Kogaku Kaishi/Journal of the Japan Society for Precision Engineering 85 (10) (2019) 856–865, https://doi.org/10.2493/JJSPE.85.856.
[11] M. Rakesh, S. Datta, Machining of Inconel 718 using coated WC tool: effects of cutting speed on chip morphology and mechanisms of tool wear, Arabian J. Sci. Eng. 45 (2) (Feb. 2020) 797–816, https://doi.org/10.1007/S13369-019-04171-4.
[12] P.A. Dearnley, E.M. Trent, Wear mechanisms of coated carbide tools, Met. Technol. 9 (1) (Feb. 1982) 60–75, https://doi.org/10.1179/030716982803285909.
[13] P.A. Dearnley, V. Thompson, A.N. Grearson, Machining ferrous materials with carbides coated by chemical vapour deposition II: wear mechanisms, Surf. Coat.

Technol. 29 (3) (Nov. 1986) 179–205, https://doi.org/10.1016/0257-8972(86)90012-5.
[14] G.K.L. Goh, L.C. Lim, M. Rahman, S.C. Lim, Transitions in wear mechanisms of alumina cutting tools, Wear 201 (1–2) (Dec. 1996) 199–208, https://doi.org/10.1016/S0043-1648(96)07238-9.
[15] M. Fallqvist, M. Nilsson, and R. M. Saoubi, Abrasive Wear of CVD α -Al2O3 and Ti (C,N) Coatings at Room and Elevated Temperature, 16th Nordic Symposium on Tribology (2014).
[16] S. Ruppi, Enhanced performance of α-Al2O3 coatings by control of crystal orientation, Surf. Coat. Technol. 202 (17) (2008) 4257–4269, https://doi.org/10.1016/j.surfcoat.2008.03.021.
[17] R. M'Saoubi, O. Alm, J.M. Andersson, H. Engström, T. Larsson, M.P. Johansson-Jõesaar, M. Schwind, Microstructure and wear mechanisms of texture-controlled CVD ʌ-Al2O3 coatings, Wear 376 (377) (2017) 1766–1778, https://doi.org/10.1016/j.wear.2017.01.071.
[18] R. Bejjani, S. Odelros, S. Öhman, M. Collin, Shift of wear balance acting on CVD textured coatings and relation to workpiece materials, Proc. IME J. J. Eng. Tribol. 235 (1) (2021) 114–128, https://doi.org/10.1177/1350650120926781.
[19] A. Bjerke, A. Hrechuk, F. Lenrick, R. M'Saoubi, H. Larsson, A. Markström, T. Björk, S. Norgren, J.E. Ståhl, V. Bushlya, Onset of the Degradation of CVD α-Al2O3 Coating during Turning of Ca-Treated Steels, Wear, Mar. 2021, 203785, https://doi.org/10.1016/j.wear.2021.203785.
[20] N. Matsui, K. Watari, Wear reduction of carbide tools observed in cutting Ca-added steels for machine structural use, ISIJ Int. 46 (11) (2006) 1720–1727, https://doi.org/10.2355/ISIJINTERNATIONAL.46.1720.
[21] A. Bjerke, F. Lenrick, S. Norgren, H. Larsson, A. Markström, R. M'Saoubi, I. Petrusha, V. Bushlya, Understanding wear and interaction between CVD α-Al2O3 coated tools, steel, and non-metallic inclusions in machining, Surf. Coat. Technol. 450 (Nov. 2022), 128997, https://doi.org/10.1016/J.SURFCOAT.2022.128997.
[22] S. Shoja, S. Norgren, H.O. Andrén, O. Bäcke, M. Halvarsson, On the influence of varying the crystallographic texture of alumina CVD coatings on cutting performance in steel turning, Int. J. Mach. Tool Manufact. 176 (May 2022), https://doi.org/10.1016/J.IJMACHTOOLS.2022.103885.
[23] A.D. Sosa, V. Collado-Ciprés, J.L. Garcia, E.L. Dalibon, L. Escalada, J. J- Roa, F. Soldera, S.P. Brühl, L. Llanes, S. Simison, Contact fatigue behavior of α-Al2O3-Ti (C,N) CVD coated WC-Co under dry and wet conditions, Mater. Lett. 284 (Feb. 2021), 129012, https://doi.org/10.1016/J.MATLET.2020.129012.
[24] N. Tamil Alagan, P. Zeman, V. Mara, T. Beno, A. Wretland, High-pressure flank cooling and chip morphology in turning Alloy 718, CIRP J Manuf Sci Technol 35 (Nov. 2021) 659–674, https://doi.org/10.1016/J.CIRPJ.2021.08.012.
[25] A. Vereschaka, S. Grigoriev, N. Sitnikov, G. Oganyan, A. Aksenenko, A. Batako, Delamination and Longitudinal Cracking in Multilayered Composite Nanostructured Coatings and Their Influence on Cutting Tool Wear Mechanism and Tool Life," Novel Nanomaterials - Synthesis and Applications, Dec. 2017, https://doi.org/10.5772/INTECHOPEN.72257.
[26] J. Rech, A. Giovenco, C. Courbon, F. Cabanettes, Toward a new tribological approach to predict cutting tool wear, CIRP Annals 67 (1) (Jan. 2018) 65–68, https://doi.org/10.1016/J.CIRP.2018.03.014.
[27] A. la Monaca, D.A. Axinte, Z. Liao, R. M'Saoubi, M.C. Hardy, Towards understanding the thermal history of microstructural surface deformation when cutting a next generation powder metallurgy nickel-base superalloy, Int. J. Mach. Tool Manufact. (Jun. 2021), 103765, https://doi.org/10.1016/J.IJMACHTOOLS.2021.103765.
[28] R. M'Saoubi, S. Ruppi, Wear and thermal behaviour of CVD α-Al2O3 and MTCVD Ti(C,N) coatings during machining, CIRP Ann.-Manuf. Technol. 58 (1) (Jan. 2009) 57–60, https://doi.org/10.1016/j.cirp.2009.03.059.
[29] D.M. D'Addona, S.J. Raykar, Thermal modeling of tool temperature distribution during high pressure coolant assisted turning of Inconel 718, Materials 12 (3) (Jan. 2019), https://doi.org/10.3390/MA12030408.